

# Parasitic Beam-Beam Perturbation for Injection Configurations in Bunch Trains

Chuang Zhang\*

## Abstract

Electron and positron bunches are separated vertically by means of electrostatic separators in LEP during injection and ramping for bunch trains. The parasitic beam-beam collisions make focusing (or defocusing) and deflection for the opposite bunches. The orbit perturbation is insignificant for injection while the parasitic beam-beam focusing (or defocusing) cause the splits of tunes, chromaticities and  $\beta$ -beatings for different bunches. In this note, two injection configurations, namely L21P20 and L21P46, are considered. Simulation with MAD shows the perturbation in these two cases is tolerable. However, care has to be taken during the injection and ramping in order to avoid resonance and instability.

Geneva, Switzerland

March 30, 1995

---

\*on leave of absence from IHEP, Beijing, China

# 1 Introduction

Tune and chromaticity splits in physics configurations of bunch trains are discussed in [1] and [2]. During injection and ramping of bunch trains, electron and positron bunches are separated by means of electrostatic separators. Fig. 1 and Fig. 2 display the vertical separation bumps of both electrons (dashed line) and positrons (solid line) at 20 GeV for L21P20 near Pit1 and Pit2 respectively. The bumps in the other odd and even pits are similar to Pit1 and Pit2 correspondingly. The directions of the eight vertical separation bumps are  $+---+---+$ . The bumps have the same direction on the left and right of each pit. For L21P46, the bumps are similar to those of L21P20. However, as the energy increases from 20 GeV to 45.6 GeV, the bump size reduces by a factor of  $20/45.6$ .

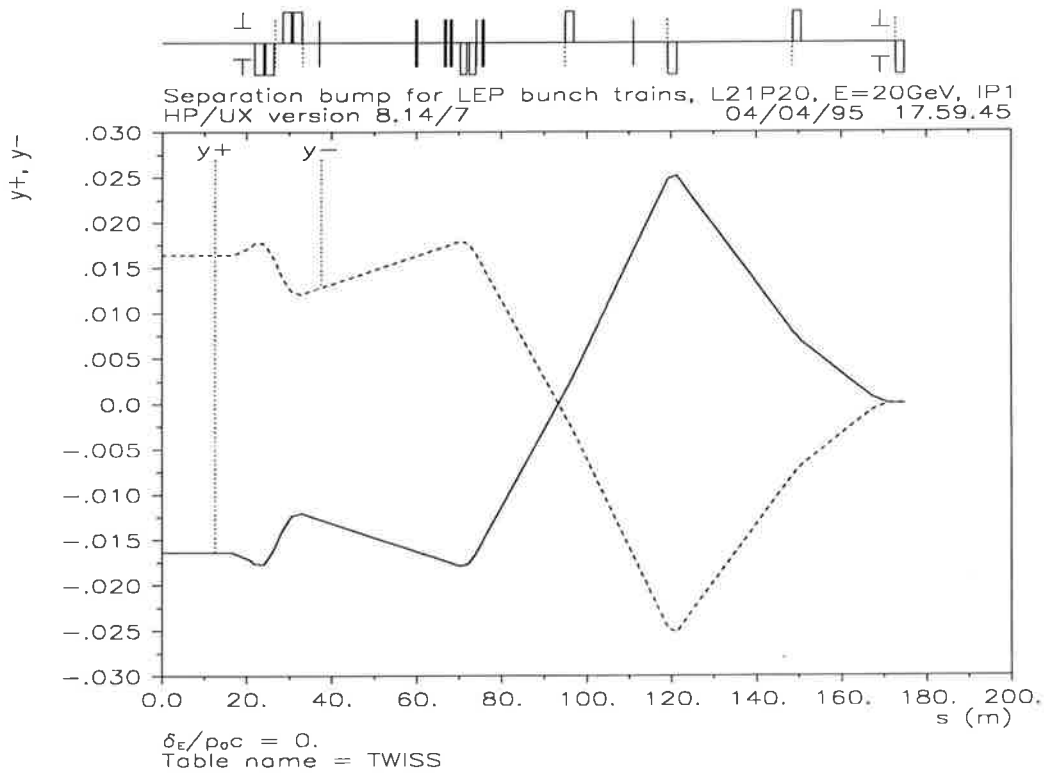


Figure 1: Vertical separation bump of electrons (dashed line) and positrons (solid line) near Pit1 in LEP for the optics L21P20 at 20 GeV

In the simulation, we assume the bunch populations  $N = 2.78 \times 10^{11}$ , corresponding to a bunch current  $I_b = 0.5$  mA in LEP. The fields of the bunch train separators taken in the MAD simulation are listed in Table 1. The principle of the choice for the fields is to keep the minimum ramping of the separator fields during the squeezing. The separator fields in the odd pits are the same as those for L05P46, which were optimized for reducing the vertical dispersion and crossing angle. The fields of ZVL7 in Pit4 and Pit8 take their maximum values of 0.19 MV,

## 2 Parasitic beam-beam perturbation

The short vertical lines in the figures indicate the parasitic collision points of four uniformly spaced bunches in each train. The parasitic beam-beam collisions make focusing (or defocusing) and deflection for the opposite bunches. In the case of separation bump  $y$  much larger than the beam size, the expressions of the effective focusing strength can be simplified as

$$k_{x,y} = \pm \frac{Nr_e}{2\pi\gamma y^2} \quad (1)$$

where  $N$  is the particle population in the bunch,  $r_e$  is the classical electron radius and  $\gamma$  is the relativistic energy. The sign in Eq.(1) denotes focusing (plus sign, on horizontal plane) or defocusing (minus sign, on vertical plane).

The parasitic beam-beam focusing (or defocusing) changes tunes, chromaticities and causes  $\beta$ -beating. As different bunches in the trains meet the opposite bunches at different positions, undergoing different perturbations, they have different tunes, chromaticities and  $\beta$ -beating. These differences can not be corrected by static field, and need to be examined whether or not they are tolerable.

When electron and positron bunches encounter each other, the beam-beam force also leads to a vertical deflection:

$$y' = -\frac{Nr_e}{\gamma y} \quad (2)$$

The beam-beam kicks perturb the vertical closed orbit and change the bump size in the parasitic collision. However, the effect is rather small and we just take it into account in MAD [3] simulation in a self-consistent manner.

## 3 Self-consistent simulation with MAD

Parasitic beam-beam perturbation calculated with Eq.(1) and Eq.(2) needs the knowledge of the bump size  $y$ , while the perturbation itself changes the bunch offsets. The new version of MAD makes the iteration possible to use the offsets at the parasitic collision points in a subsequent TWISS command, and to repeat this until convergence is obtained [4]. Table 2 shows the results of MAD simulation for parasitic beam-beam perturbation in different iterations, taking bunch "a" (leading one) in optics L21P46 at 45.6 GeV as an example.

It can be seen from Table 2 that the parameters are well converged after a few iterations. The simulation with 10 iterations in our study should be well self-consistent. To compare the orbit data listed in Table 2 with their unperturbed values of  $y_{0,max} = 14.434060$  mm,  $y_{0,rms} = 2.305526$  mm, the parasitic beam-beam collisions cause only a fractional change of the vertical orbits.

## 5 Parasitic beam-beam perturbation for L21P46

As  $k \propto \gamma^{-1}y^{-2} \propto \gamma$  for the same separator field, the perturbation is expected to be larger roughly by a factor of  $45.6/20 = 2.28$  in the L21P46 case than in L21P20. Table 3 gives the results of MAD simulation.

Table 4 Parasitic beam-beam perturbation to bunches in trains  
for injection configuration at 45.6 GeV

Bunch	$Q_x$	$Q_x$	$Q'_x$	$Q'_y$	$\beta_{x,max}$ (m)	$\beta_{y,max}$ (m)
O	90.289113	76.194192	1.004030	0.995667	312.614853	189.247773
a	90.322638	76.173779	0.732440	1.587373	317.250550	200.782938
b	90.328774	76.182043	0.911047	1.056352	310.862410	192.247780
c	90.329526	76.181681	0.905506	1.085853	310.740196	193.392104
d	90.323817	76.173266	0.745965	1.384752	316.766793	198.451074
S	0.006888	0.008777	0.178607	0.531021	6.510354	8.535158

In comparison with the L21P20 case in Table 3, the  $\delta Q_{x,max}$ ,  $\delta Q_{y,max}$ ,  $\delta Q'_{x,max}$ ,  $\delta Q'_{y,max}$ ,  $\delta\beta_{x,max}$  and  $\delta\beta_{y,max}$  in L21P46 increase by the factors of 2.45, 1.92, 1.93, 2.06, 2.35 and 2.20 respectively, which is in a good agreement with the above analysis. As the instability threshold gets higher at the higher energy, these amounts of increment of perturbation can be considered to be safe.

## 6 Conclusions

The parasitic beam-beam perturbation for the injection configurations L21P20 and L21P46 is simulated with the new version of MAD in a consistent manner. The results are understandable and explainable.

The  $\beta$ -beating caused by the parasitic beam-beam collisions is small, while the orbit perturbation is insignificant. The tune splits ( $\delta Q_{x,max} = 0.0028$ ,  $\delta Q_{y,max} = 0.0046$  at 20 GeV and  $\delta Q_{x,max} = 0.0069$ ,  $\delta Q_{y,max} = 0.0088$  at 45.6 GeV) and chromaticity splits ( $\delta Q'_{x,max} = 0.092$ ,  $\delta Q'_{y,max} = 0.26$  at 20 GeV and  $\delta Q'_{x,max} = 0.18$ ,  $\delta Q'_{y,max} = 0.53$  at 45.6 GeV) are tolerable.

Nevertheless, the splits are not negligible. One needs to adjust the tune and chromaticity in order to optimize the performance of injection and ramping in LEP bunch train operation.

## Acknowledgements

The author wish to thank E. Keil for the discussion on the self-consistent simulation with MAD and the comments on the draft of this paper.